

# A neuromarker for drug and food craving distinguishes drug users from non-users

Received: 26 July 2021

Accepted: 1 November 2022

Published online: 19 December 2022

 Check for updates

Leonie Koban <sup>1,4</sup>✉, Tor D. Wager <sup>2,5</sup>✉ & Hedy Kober <sup>3,5</sup>✉

Craving is a core feature of substance use disorders. It is a strong predictor of substance use and relapse and is linked to overeating, gambling, and other maladaptive behaviors. Craving is measured via self-report, which is limited by introspective access and sociocultural contexts. Neurobiological markers of craving are both needed and lacking, and it remains unclear whether craving for drugs and food involve similar mechanisms. Across three functional magnetic resonance imaging studies ( $n = 99$ ), we used machine learning to identify a cross-validated neuromarker that predicts self-reported intensity of cue-induced drug and food craving ( $P < 0.0002$ ). This pattern, which we term the Neurobiological Craving Signature (NCS), includes ventromedial prefrontal and cingulate cortices, ventral striatum, temporal/parietal association areas, mediodorsal thalamus and cerebellum. Importantly, NCS responses to drug versus food cues discriminate drug users versus non-users with 82% accuracy. The NCS is also modulated by a self-regulation strategy. Transfer between separate neuromarkers for drug and food craving suggests shared neurobiological mechanisms. Future studies can assess the discriminant and convergent validity of the NCS and test whether it responds to clinical interventions and predicts long-term clinical outcomes.

Craving—a strong desire to use drugs or to eat—has long been considered a core factor driving overeating and substance use<sup>1</sup>, thereby contributing to the top three preventable causes of disease and death<sup>2</sup>. In 2013, it was added as a diagnostic criterion for substance use disorders (SUDs) in the *Diagnostic and Statistical Manual of Mental Disorders, Fifth Edition*<sup>3</sup>, underscoring its clinical significance. Importantly, cue-induced craving, which arises in response to drug-related or food-related stimuli, is known to prospectively predict eating unhealthy foods (that is, ultra-processed foods high in sugar and saturated fat), weight gain, drug use and relapse (for meta-analyses, see refs. <sup>4–6</sup>). Because it is a common predictor across multiple conditions (including SUDs, obesity, and eating disorders) and maladaptive behaviors, it may constitute a transdiagnostic risk factor.

Although self-reported craving has been useful clinically as well as experimentally, there is growing recognition of the need to understand its biological basis. Human neuroimaging studies have identified circuits related to substance use risk, incidence, and sequelae<sup>7,8</sup>. Some circuits, including ventromedial prefrontal cortex (vmPFC), ventral striatal/nucleus accumbens (VS/NAc) and insula, have been identified across SUDs, outcomes, and risky behaviors, and have been identified as key regions underlying addiction in animal models<sup>9–13</sup>. Alongside homeostatic circuits in hypothalamus and brainstem, these regions have been identified in studies of food valuation and dietary decision-making<sup>14,15</sup> and appear to be functionally related to weight gain and obesity<sup>16,17</sup>. These circuits can be targeted by neurostimulation, pharmacological, psychological, and behavioral interventions<sup>18</sup>, providing new avenues for therapeutic intervention.

<sup>1</sup>Paris Brain Institute (ICM), Inserm, CNRS, Sorbonne Université, Paris, France. <sup>2</sup>Department of Psychological and Brain Sciences, Dartmouth College, Hanover, NH, USA. <sup>3</sup>Department of Psychiatry and Psychology, Yale University, New Haven, CT, USA. <sup>4</sup>Centre de Recherche en Neurosciences de Lyon (CRNL), CNRS, INSERM, Université Claude Bernard Lyon 1, Bron, France. <sup>5</sup>These authors contributed equally: Tor D. Wager, Hedy Kober.

✉ e-mail: [leonie.koban@cnrs.fr](mailto:leonie.koban@cnrs.fr); [tor.d.wager@dartmouth.edu](mailto:tor.d.wager@dartmouth.edu); [hedy.kober@yale.edu](mailto:hedy.kober@yale.edu)

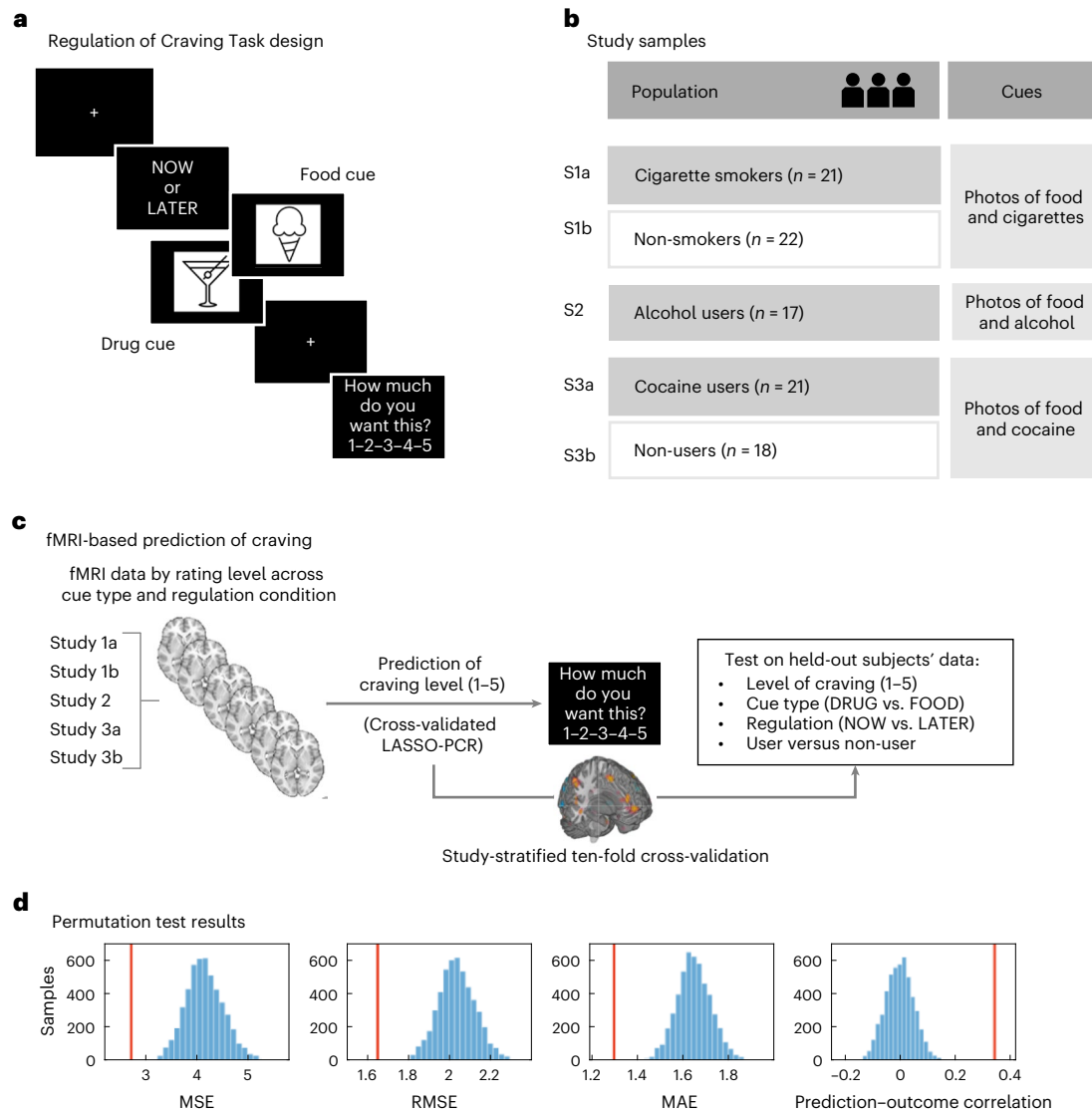


**Fig. 1 | Study design and analytic approach.** **a**, In the Regulation of Craving task, participants were presented with a series of photographs depicting either drugs (cigarettes, alcoholic drinks or cocaine) or highly palatable food items (cigarettes, alcoholic drinks or cocaine) or highly palatable food items (cigarettes, alcoholic drinks or cocaine) or highly palatable food items (cigarettes, alcoholic drinks or cocaine). Before presentation of the cues, participants were instructed (2-second written cue) to consider either the immediate consequences of consumption of the items ('NOW' condition) or their negative (typically long-term) consequences ('LATER' condition). At the end of each trial, participants rated their craving ('How much do you want this?') using a 1–5 Likert scale. **b**, The present study employed the pooled data from three previous studies (five groups of participants). Study 1 tested the Regulation of Craving task (displaying cigarette and food cues) in 21 heavy smokers (Study 1a) and 22 non-smokers (Study 1b; see details in Methods). Study 2 tested the Regulation of Craving task (displaying alcohol and food cues) in participants fulfilling diagnostic criteria of alcohol use disorder ( $n = 17$ ; see details in Methods). Study 3 tested the Regulation of Craving task (displaying

cocaine and food cues) in 21 individuals with cocaine use disorder (Study 3a) and 18 matched non-users (Study 3b; see details in Methods). **c**, For each participant from all five studies, we computed brain activation images ( $\beta$ -estimates) for each level of craving (1–5). These images were then used in a LASSO-PCR machine learning algorithm to predict level of craving (1–5) based on brain activity. Cross-validation (ten-fold stratified for studies and participant populations) allowed assessment of (1) predictive accuracy of the pattern for craving; (2) whether it was differentially activated for drug versus food cues; (3) whether it was differentially activated for the two regulation conditions (NOW versus LATER); and (4) whether the pattern can differentiate drug users from non-users. **d**, Permutation test results. Null distributions are plotted in blue bars, observed accuracy measures as red lines. For all measures, none of the permutation samples performed as well as the observed results (all  $P < 0.0002$ ). MAE, mean absolute error; MSE, mean squared error; RMSE, root-mean-square error.

Nevertheless, although great strides have been made in the understanding of substance misuse, overeating and related phenomena, understanding of the neural basis of craving is still incomplete, and neural targets for monitoring craving and SUDs and for examining the efficacy of interventions are lacking. Although the neuroimaging literature on craving is growing, craving cannot be directly measured in non-humans<sup>19</sup>. In addition, understanding that any specific brain region is involved in craving or other outcomes does not imply that we can decode craving from the brain or that we have a sufficiently precise measurement model to allow for monitoring of individual people or

testing whether treatments engage their intended craving-related neural targets<sup>20</sup>. It is increasingly apparent that many mental states and related outcomes have a highly distributed brain basis, including emotion<sup>21,22</sup>, pain<sup>23</sup>, perception<sup>24</sup>, object recognition<sup>25</sup>, memory retrieval<sup>26</sup>, sustained attention<sup>27</sup>, semantics<sup>28</sup>, and autonomic responses<sup>29</sup>. Accordingly, measures that integrate across brain systems can provide sensitive, specific, and generalizable characterizations of the neurophysiological underpinnings of behavior<sup>30</sup>. They can also predict health-related outcomes with larger effect sizes than measures based on single regions, in many cases<sup>31</sup>.

Such predictive models—also called ‘neuromarkers’ or ‘signatures’—have multiple potential uses<sup>32–34</sup>. They can predict risk for future disorders, identify subtypes (or biotypes) that predict who will respond to a treatment, and, perhaps most importantly, serve as mechanistic targets for interventions. They can also outperform subjective measures in predicting human choices<sup>35</sup> and can be linked with systems and cellular neuroscience to develop new biological treatments in ‘reverse translation’ approaches<sup>19</sup>. Accordingly, there is increasing recognition of the need to develop biomarkers based on human systems that can be compared with animal models<sup>33,34,36</sup>. However, such an approach has rarely been applied in addiction<sup>37</sup> and has not yet been applied to craving.

In this study, we took a first step toward a neuromarker that predicts the intensity of drug and food craving in clinical and matched control samples. We integrated data from five different cohorts in three functional magnetic resonance imaging (fMRI) studies across different types of drug users (cigarettes, alcohol and cocaine) and non-users (a total of 469 contrast images from  $n = 99$  participants). Across studies, participants were presented with visual cues of drugs and highly palatable food items. We then used machine learning to identify a distributed functional brain activity pattern that predicted the intensity of craving.

We term the resulting pattern the Neurobiological Craving Signature (NCS), and we hope that this name reduces ambiguity and provides a reference point for the pattern’s future reuse and testing in new samples. Analyses related to the NCS allow us to address scientific questions related to the organization of craving-related brain systems across drugs and food (or other rewarding stimuli) and their susceptibility to cognitive, pharmacological and other interventions. Furthermore, recent perspectives have proposed a common neurophysiology for SUDs and obesity and of drug and food craving more specifically<sup>38–40</sup>, but this view has been challenged<sup>41</sup>. The NCS allows us to test whether craving for several types of drugs, including stimulants (nicotine and cocaine) and sedatives (alcohol), and for highly palatable foods are based on different or shared neurophysiological patterns. We further assess whether the brain systems involved in cue-induced craving are affected by cognitive regulation strategies, highlighting the malleability of craving-related brain patterns to interventions and, thus, opening avenues for developing further interventions and improving existing ones.

## Results

### Data overview

A total of 469 contrast images from 99 participants and five independent cohorts were used for training and testing the pattern to predict drug and food craving (two drug-using cohorts, two of their matched controls and another sample of drug users with no matched controls). All participants viewed images of drugs and food under two instruction conditions: a craving instruction and an instruction to use a cognitive strategy to reduce craving (Methods). Contrast images were computed for the onset of the visual drug and food cues (Fig. 1a) separately for each level of craving (1–5 Likert scale) for every participant (Supplementary Fig. 1) and were rescaled by the image-wise L2 norm to remove any differences in scale between participants and scanners.

### fMRI results

**Description of the NCS.** Parallel to previous studies on fMRI-based prediction of pain and emotion<sup>21,23</sup>, least absolute shrinkage and selection operator–principal component regression (LASSO–PCR) and study-stratified ten-fold cross-validation was used to predict the level of craving based on fMRI contrast images. The advantage of this approach is that it does not require a similar level of craving across food and drugs (or across participants and studies), because it predicts continuous, dimensional craving intensity ratings. Variance in self-reported craving, both within and between participants, is beneficial for the LASSO–PCR

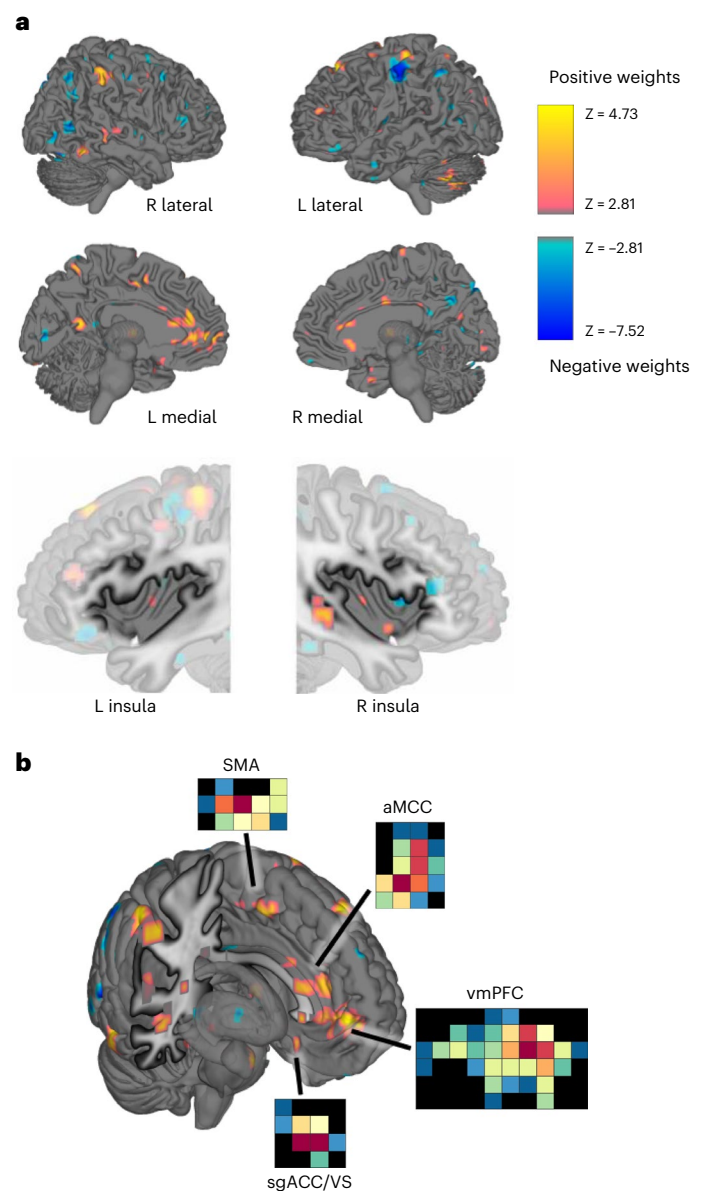


**Fig. 2 | Thresholded display of the NCS.** Note that unthresholded patterns are used for prediction; this thresholded pattern is shown for illustration at  $P < 0.005$  uncorrected. **a**, Medial, lateral and insula displays of the most consistent pattern weights. **b**, Pop-out rectangles show the multivariate pattern for selected clusters of interest. Warm (yellow-red) color indicates positive weights; cold (cyan-purple) color indicates negative weights in predicting drug and food craving.  $P$  values are based on bootstrapping and indicate the areas that contribute most consistently with positive or negative weights. See Table 1 for a list of FDR-corrected weights. The NCS weight map and code to apply it to new data are available for download at [https://github.com/canlab/Neuroimaging\\_Pattern\\_Masks/tree/master/Multivariate\\_signature\\_patterns/2022\\_Koban\\_NCS\\_Craving](https://github.com/canlab/Neuroimaging_Pattern_Masks/tree/master/Multivariate_signature_patterns/2022_Koban_NCS_Craving). aMCC, anterior midcingulate cortex; sgACC, subgenual anterior cingulate cortex; SMA, supplementary motor area.

algorithm. Model training identifies a pattern of weights across voxels such that the weighted average activity is optimized to predict craving in a training sample of participants, and its predictive accuracy is validated in independent participants. The NCS is a model that consists of the weights (plus an overall intercept), which can be applied to any brain image to obtain a weighted average over brain voxels, yielding a single score per test image. If weights in a brain area are positive, more activity indicates higher predicted craving; if they are negative, more

**Table 1 | Clusters of FDR-corrected bootstrapped weights of the NCS**

Region name	Volume (mm <sup>3</sup> )	x	y	z	Max(z)	Atlas region (see note)	Large-scale network/structure (see note)
<b>Positive weights</b>							
Postcentral gyrus/somatosensory cortex	405	-42	-27	60	4.7279	3b L	SomatomotorA
Inferior temporal gyrus	189	57	-48	-15	4.6653	TE1p R	Fronto Parietal B
Cerebellum	297	-48	-63	-39	4.659	Cblm Crusl L	Cerebellum
Subcallosal gyrus/ventral striatum	135	12	6	-21	4.5203	pOFC R	Limbic
Superior frontal gyrus/dorsolateral prefrontal cortex	270	-24	33	54	4.4567	8BL L	Default Mode B
Rostral gyrus/vmPFC	162	-6	51	3	4.3707	a24 L	Default Mode A
Retrosplenial cortex	27	-3	-54	15	4.2439	v23ab L	Default Mode A
Inferior parietal lobule	108	30	-63	45	4.235	IP1 R	Dorsal Attention A
Supramarginal gyrus	54	57	-33	45	4.2191	PF R	Ventral Attention A
Supraparietal lobule	27	-12	-60	60	4.0332	7Am L	Dorsal Attention B
Thalamus	108	0	-9	6	4.0137	Thal MD	Diencephalon
Angular gyrus	27	57	-36	21	3.9646	PSL R	Temporal Parietal
Middle frontal gyrus	27	-42	39	18	3.8987	46 L	Ventral Attention B
Lateral occipital	27	51	-72	-18	3.8826	PH R	Dorsal Attention A
<b>Negative weights</b>							
Postcentral gyrus/somatosensory cortex	2025	-51	-21	51	-7.5193	1 L	Somatomotor A
Middle temporal gyrus	243	54	-63	6	-4.8288	TPOJ2 R	Dorsal Attention A
Superior occipital gyrus	108	18	-84	45	-4.5147	V6A R	Visual Peripheral
Angular gyrus	162	42	-60	33	-4.5105	Pgi R	Default Mode C
Visual cortex	81	39	-72	-18	-4.4118	PIT R	Visual Central
Superior temporal gyrus	27	54	-3	0	-4.187	Pbelt R	Somatomotor B
Precuneus	27	9	-63	33	-4.052	POS2 R	Fronto Parietal C
Superior parietal lobule	27	-12	-57	75	-3.9052	7AL L	Dorsal Attention B
Visual cortex	27	0	-84	6	-3.8653	V1 R	Visual Peripheral
Angular gyrus	27	-51	-60	54	-3.8516	PFm L	Fronto Parietal B

Note: Significant positive and negative weights contributing to the NCS (FDR-corrected  $q < 0.05$  across the whole-brain gray matter mask). Cortical atlas regions are labeled based on a combination of parcellations available on GitHub (see Methods for details): [https://github.com/canlab/Neuroimaging\\_Pattern\\_Masks/tree/master/Atlases\\_and\\_parcellations/2018\\_Wager\\_combined\\_atlas](https://github.com/canlab/Neuroimaging_Pattern_Masks/tree/master/Atlases_and_parcellations/2018_Wager_combined_atlas). This repository includes multiple atlases and other meta-analytic and multivariate maps. Tools for manipulating and analyzing this and other atlases are in the CANlab Core Tools repository: <https://github.com/canlab/CanlabCore>.

activity indicates lower predicted craving. Figure 2 presents a thresholded display of the resulting weight map based on bootstrapping. Although the unthresholded map (Supplementary Fig. 2) is used for prediction, the thresholded map illustrates the brain areas that most robustly contribute positive or negative weights to the predictive pattern. Areas with positive weights included vmPFC, dorsal anterior cingulate cortex, subgenual cingulate/ventral striatum, retrosplenial cortex, parietal and temporal areas, cerebellum and amygdala. Negative weights were found in visual areas, lateral prefrontal and parietal and somatomotor areas, among others (see Table 1 for a list of false discovery rate (FDR)-corrected coordinates). Of note, many areas, including somatomotor cortex, parietal and temporal cortex, and bilateral insula, included clusters of both positive and negative weights.

**Predictive performance of the NCS.** The trained pattern resulted in a cross-validated prediction–outcome correlation of  $r = 0.53$  (standard deviation  $\pm 0.46$ ) within-person and  $r = 0.34$  across all data points, with a mean absolute error of 1.30 points on the 1–5 Likert scale. A multi-level general linear model (GLM) confirmed a strong relationship between out-of-sample predicted and actual level of craving with a large effect size ( $\beta = 0.38$ , standard error [STE] = 0.04,  $t(98) = 9.21$ ,  $P < 0.0001$ ,

Cohen's  $d = 0.93$ ; Fig. 3). The strength of the predictive performance varied across datasets but was significant in all five cohorts, with effect sizes (Cohen's  $d$ ) ranging from 0.55 to 1.48 (Table 2). Statistically controlling for white matter and ventricle signal did not alter these results (that is, the relationship between craving ratings and NCS remained significant ( $\beta = 0.35$ , STE = 0.05,  $t(97) = 6.81$ ,  $P < 0.0001$ ), whereas the relationship of white matter and ventricle signals with craving was not ( $\beta = 2.53$ , STE = 1.77,  $t(97) = 1.43$ ,  $P = 0.16$ ). Adding scanner site, group (drug users versus controls), sex, age, education, body mass index and average head motion as second-level covariates also did not alter the relationship between craving and NCS ( $\beta = 0.38$ , STE = 0.04,  $t(79) = 9.17$ ,  $P < 0.0001$ ). Although the NCS predicts craving in both users and non-users, users versus non-users had significantly higher overall NCS responses ( $\beta = 0.38$ , STE = 0.18,  $t(79) = 2.13$ ,  $P = 0.036$ ) and smaller effect of craving ratings on out-of-sample NCS-predicted responses (that is, a smaller slope,  $\beta = -0.14$ , STE = 0.05,  $t(79) = -2.97$ ,  $P = 0.004$ ), potentially because users may report ratings less reliably or have less neurotypical brains. None of the other covariates significantly affected the NCS or interacted with ratings to affect NCS responses. NCS responses did not significantly change over time during the experiment (Supplementary Fig. 3).

**Table 2 | Predictive performance of the NCS and effect sizes for each study sample**

Dataset	Cues	Sample	n	Prediction-outcome (glmfit_multilevel)	Effect size (Cohen's d)
Study 1a	Cigarette and food cues	Cigarette smokers	21	$\beta=0.22$ , STE=0.09, $t(20)=2.45$ , $P=0.024$	$d=0.55$
Study 1b	Cigarette and food cues	Non-smokers	22	$\beta=0.46$ , STE=0.07, $t(21)=6.77$ , $P<0.001$	$d=1.48$
Study 2	Alcoholic drinks and food cues	Alcohol users	17	$\beta=0.32$ , STE=0.11, $t(16)=2.76$ , $P=0.014$	$d=0.69$
Study 3a	Cocaine and food cues	Cocaine users	21	$\beta=0.36$ , STE=0.09, $t(20)=3.87$ , $P=0.001$	$d=0.87$
Study 3b	Cocaine and food cues	Non-users	18	$\beta=0.58$ , STE=0.09, $t(17)=6.11$ , $P<0.001$	$d=1.48$
All studies			99	$\beta=0.38$ , STE=0.04, $t(98)=9.21$ , $P<0.001$	$d=0.93$

**Classification of high versus low craving.** We next assessed the accuracy of the NCS to differentiate between high versus low levels of craving. Forced-choice binary classification of highest versus lowest levels of craving per participant was achieved with a cross-validated accuracy of 81%  $\pm$  4.0% STE, binomial test  $P < 0.0001$  (sensitivity = 81%, specificity = 81%, area under the curve (AUC) = 0.91; Fig. 3). Even across participants (single-interval classification), this pattern separated brain responses to the highest versus lowest individual levels of craving with 72% cross-validated accuracy ( $\pm$  3.4% STE, binomial test  $P < 0.0001$ , sensitivity = 64%, specificity = 80%, AUC = 0.76). Although this level of predictive accuracy does not provide perfect separation of high versus low craving, it is remarkable, because all stimuli were drugs or highly palatable food items; thus, differences in classification performance were not driven by external stimulus characteristics but by the personal history and internal motivational states of the participants.

Our studies did not include in-scanner ratings other than craving ratings. We, therefore, assessed whether the NCS does indeed predict something specific to craving that is not predicted by other brain signatures, which are trained to predict other types of affect ratings. For this purpose, we applied five recently developed brain signatures<sup>42</sup>—trained to predict four different types of negative affect (mechanical pain, thermal pain, aversive sounds and unpleasant pictures) and domain-general negative affect—to the data from Studies 1–3 and tested whether these other brain signatures would predict high versus low craving with similar accuracy as the NCS. The results of this control analysis confirmed that other signatures trained to predict affective ratings did not significantly predict high versus low cravings but were at chance level (46–52% accuracy; Supplementary Fig. 4).

**Differentiating drug users from non-users.** We next tested whether individual craving pattern responses to drug and food cues could be used to predict whether a participant was a drug user or a non-user (see Fig. 4a for group averages, Fig. 4b for individual effects and Fig. 4c for receiver operating characteristic plots). Although pattern expression

in brain responses to food cues did not significantly differentiate drug users from non-users (60% accuracy  $\pm$  4.9% STE,  $P = 1.00$ , AUC = 0.40), NCS pattern responses to drug cues significantly classified drug users from non-users, with 75% accuracy ( $\pm$  4.4% STE,  $P = 0.002311$ , sensitivity = 86%, specificity = 57%, AUC = 0.76). When testing the pattern response to the drug > food contrast, the response in the NCS separated drug users from non-users with 82% accuracy ( $\pm$  3.9% STE,  $P < 0.001$ , sensitivity = 97%, specificity = 60%, AUC = 0.87; Fig. 4c).

Given slight but significant differences in years of education between users and non-users, we used a GLM to control for years of education and other basic demographic variables (age and biological sex) in predicting individual differences in NCS response. This showed that drug users had stronger NCS responses to drug cues than non-users ( $t(94) = 4.22$ ,  $P < 0.001$ , 96% confidence interval (CI): 0.57, 1.55, Cohen's  $d = 0.87$ ) and stronger NCS responses to drug > food cues ( $t(94) = 7.04$ ,  $P < 0.001$ , 96% CI: 0.90, 1.60, Cohen's  $d = 1.45$ ), whereas education, age and sex were not associated with NCS responses to drugs or drug > food cues (all  $P > 0.20$ ).

In addition, we tested whether the classification of drug users versus non-users could be driven by any single study (or user group) alone or whether they are significant in each study independently. We performed the classification analysis separately on Studies 1 and 3 (note that Study 2 did not include non-users). The results showed that NCS responses to drug cues and drug > food cues (but not food cues) significantly separated users from non-users in both Study 1 and Study 3, separately (see Supplementary Fig. 5 for receiver operating characteristic plots and full results). Average craving ratings and NCS responses for each study and cue type are also shown in Supplementary Fig. 6.

**Drug and food cravings are predicted by shared brain patterns.** An important debate concerns the question whether drug and food cravings are based on similar brain processes<sup>39,41</sup>. If drug and food cravings are driven by shared brain processes, then drug craving should be predictable based on a pattern that is trained to predict food craving, and food craving should be predictable based on a pattern that is trained to predict drug craving—at least in drug users. Conversely, if drug and food cravings are based on dissociable brain processes, then better predictive accuracy would be gained by training drug-specific and food-specific (compared to craving-general) brain patterns.

We, therefore, repeated the procedures described above and tested whether training on drug and food data separately would improve prediction of craving and whether food craving could be predicted based on a pattern trained on drug data only and vice versa (Fig. 5). Food craving was predicted similarly well by the overall pattern (76% out-of-sample accuracy  $\pm$  4.3% STE,  $P < 0.001$ , AUC = 0.82) as by a craving pattern trained on food cues only (79%  $\pm$  4.1% STE,  $P < 0.001$ , AUC = 0.88). Food craving was also significantly predicted by a pattern trained on drug cues only but with somewhat lower accuracy across both drug-using and non-drug-using participants (65%  $\pm$  4.8% STE,  $P = 0.005$ , AUC = 0.68). For the prediction of drug craving, the results indicated no substantial improvements for training only on modality-specific (drug) cue trials (69%  $\pm$  4.9% STE,  $P < 0.001$ , AUC = 0.75) compared to all cues (70%  $\pm$  4.9% STE,  $P < 0.001$ , AUC = 0.78). Drug craving was also significantly predicted by a pattern that was trained only on food trials (66%  $\pm$  5.1% STE,  $P = 0.004$ , AUC = 0.74). Thus, we did not find evidence for a double dissociation between drug and food craving but, rather, significant cross-prediction of drug and food craving. Most notably, the NCS performed as well as the two cue-specific patterns. Together, this supports the hypothesis of shared representations between drug and food craving and across drug types.

### Modulation by cognitive regulation strategies

Finally, we used a GLM to assess how craving ratings and responses of the NCS were modulated by the cognitive Regulation of Craving task

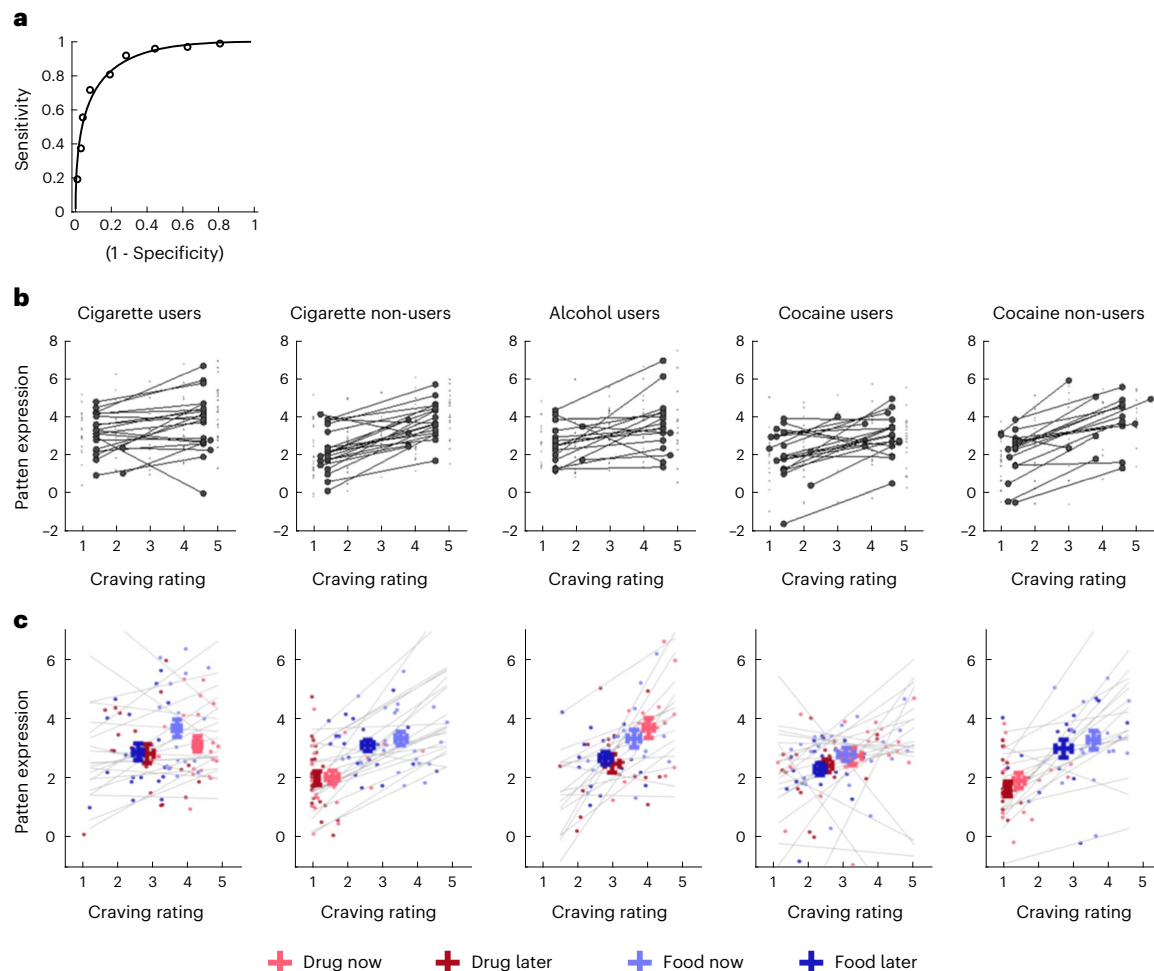


**Fig. 3 | Predictive performance of the NCS.** **a**, Receiver operating characteristic plot for the prediction of highest versus lowest levels of craving (forced-choice discrimination,  $n = 99$ ). **b**, Individual datapoints and slopes for the relationship between craving levels and NCS for all five datasets (significant positive association in each study; Table 2). **c**, Average levels of craving ratings (on the x axis) and NCS responses (on the y axis) for each of the four experimental

conditions (drug versus food cues and NOW versus LATER instruction) and within each dataset. Gray lines show individual slopes across the four conditions. Dots indicate individual data points for each condition and participant. Horizontal and vertical error bars indicate s.e.m. for ratings and NCS pattern expression, respectively (Study 1a:  $n = 21$ ; Study 1b:  $n = 22$ ; Study 2:  $n = 17$ ; Study 3a:  $n = 21$ ; Study 3b:  $n = 18$ ).

that was employed in all five studies. Across all participants, craving ratings were influenced by cue type (drug versus food,  $F_{(1,388)} = 95.5$ ,  $P < 0.001$ , 95% CI:  $-0.44, -0.29$ ) and regulation instruction (NOW versus LATER,  $F_{(1,388)} = 97.6$ ,  $P < 0.001$ , 95% CI:  $0.32, 0.49$ ). Drug users reported greater overall craving ( $F_{(1,388)} = 74.2$ ,  $P < 0.001$ , 95% CI:  $0.36, 0.58$ ), and this group effect interacted with both regulation instruction ( $F_{(1,388)} = 4.51$ ,  $P = 0.034$ , 95% CI:  $0.01, 0.17$ ) and cue type ( $F_{(1,388)} = 191.5$ ,  $P < 0.001$ , 95% CI:  $0.44, 0.59$ ), such that drug users craved drugs ( $t_{(97)} = 14.5$ ,  $P < 0.001$ , 95% CI:  $1.69, 2.23$ , Cohen's  $d = 2.94$ ) but not food ( $t_{(97)} = -0.67$ ,  $P = 0.50$ , 95% CI:  $-0.34, 0.17$ , Cohen's  $d = 0.14$ ) more than non-users and that they showed slightly higher regulation effects than non-users. Notably, these effects were qualified further by a significant three-way interaction among group, cue type and regulation condition ( $F_{(1,388)} = 21.7$ ,  $P < 0.001$ , 95% CI:  $0.05, 0.12$ ; Fig. 3c). Although the regulation effect was significant for both drug and food cues in both users and non-users, the difference between NOW and LATER condition was significantly smaller in the drug condition compared to the food condition in non-users ( $t_{(37)} = -4.22$ ,  $P < 0.001$ , 95% CI:  $-0.77, -0.27$ , Cohen's  $d = 0.67$ ), who reported low craving for drugs overall. Consistently, drug users had a somewhat larger regulation effect (difference between NOW and LATER condition) for drug compared to food cues ( $t_{(58)} = 2.14$ ,  $P = 0.037$ , 95% CI:  $0.01, 0.35$ , Cohen's  $d = 0.28$ ).

Similarly to craving ratings, responses of the NCS were influenced by cue type (drug versus food,  $F_{(1,388)} = 70.4$ ,  $P < 0.001$ , 95% CI:  $-0.51, -0.83$ ) and by regulation instruction (NOW versus LATER,  $F_{(1,388)} = 35.5$ ,  $P < 0.001$ , 95% CI:  $0.28, 0.55$ ), suggesting that cognitive regulation strategies modify NCS responses. Drug users versus non-users had marginally greater NCS responses overall ( $F_{(1,388)} = 3.0$ ,  $P = 0.085$ , 95% CI:  $-0.05, 0.75$ ). Drug users' versus non-users' signature response differed with respect to cue type ( $F_{(1,388)} = 57.5$ ,  $P < 0.001$ , 95% CI:  $0.90, 1.53$ ), such that drug users had higher NCS responses to drug cues than non-users ( $t_{(97)} = 4.39$ ,  $P < 0.001$ , 95% CI:  $0.56, 1.49$ , Cohen's  $d = 0.90$ ), whereas NCS responses to food cues did not significantly differ ( $t_{(97)} = -1.13$ ). Furthermore, drug users' versus non-users' signature response differed with respect to regulation condition ( $F_{(1,388)} = 9.15$ ,  $P = 0.003$ , 95% CI:  $0.15, 0.69$ ), such that users had larger NCS responses than non-users in the NOW condition ( $t_{(97)} = 2.53$ ,  $P = 0.013$ , 95% CI:  $0.12, 1.00$ , Cohen's  $d = 0.52$ ) but not in the LATER condition ( $t_{(97)} = 0.71$ ) (Fig. 3c), which was likely driven by more room to downregulate craving in users compared to non-users. The three-way interaction among group, regulation and cue type was not significant for NCS responses ( $F_{(1,388)} = 0.0$ ).

**Affective stimulus characteristics.** We next explored how self-reported craving and the NCS were related to intrinsic

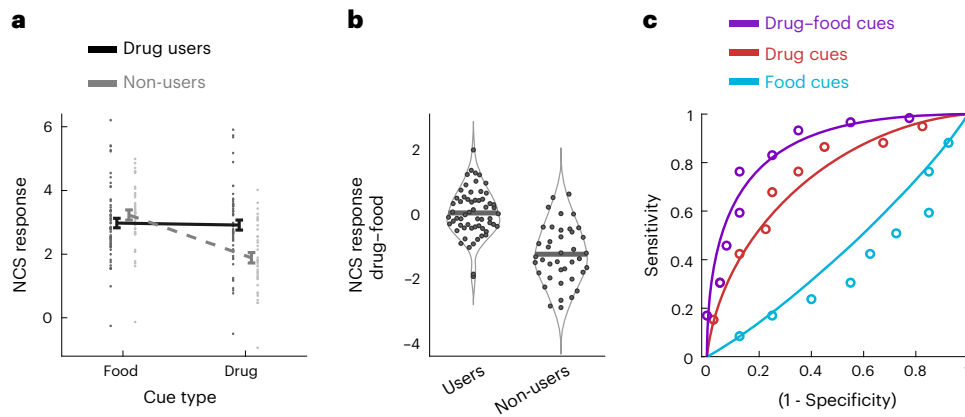


**Fig. 4 | Classification of drug users versus non-users based on NCS responses to drugs and food.** **a**, Out-of-sample responses of the NCS to drug and food cues, in drug users ( $n = 59$ ) and non-users ( $n = 40$ ). Data are presented as mean values  $\pm$  s.e.m.; dots show individual data points. **b**, Differences in NCS responses to drug minus food cues, in drug users versus non-users. **c**, Receiver operating

characteristic plots for NCS-based prediction of drug use. Whereas NCS responses to food cues did not significantly separate users from non-users (in blue), NCS responses to drug cues were able to significantly separate users from non-users (in red). Differential NCS responses to drug and food cues (in purple) had the highest classification accuracy (82%; see text for details).

craving-related image features of the different food and drug cues. For this purpose, we employed a deep learning neural network that has been previously trained to detect 20 different affective states, including craving, in visual images (‘EmoNet’<sup>43</sup>). This allowed us to test whether single-trial craving ratings and NCS responses were associated with the EmoNet visual ‘craving’ output unit on a stimulus-by-stimulus basis. EmoNet ‘craving’ output is a probability score indicating the predicted probability that humans will label an image as ‘craving’ related and reflects a high-level abstraction of visual input. A multi-level GLM confirmed that both stimulus-to-stimulus craving ratings ( $\beta = 0.04$ ,  $STE = 0.00$ ,  $t(95) = 10.5$ ,  $P < 0.001$ ) and NCS responses ( $\beta = 0.02$ ,  $STE = 0.00$ ,  $t(95) = 6.80$ ,  $P < 0.001$ ) were strongly and positively associated with the automatic EmoNet ‘craving’ scores for the stimuli (see Supplementary Fig. 7 for additional results). Notably, the association between craving ratings and NCS remained highly significant when controlling for ‘craving’ stimulus features ( $\beta = 0.18$ ,  $STE = 0.02$ ,  $t(95) = 8.60$ ,  $P < 0.001$ ), ruling out stimulus features as the main or only source of NCS variability. Instead, the NCS significantly mediated the effects of EmoNet’s ‘craving’ output on self-reported craving ( $P = 0.011$ ; Fig. 6).

**Discussion**

Craving contributes to multiple behaviors that are detrimental to physical and mental health in the long term, including smoking, alcohol drinking, overeating and gambling<sup>4,5</sup>, and is arguably one of the most central processes in SUDs<sup>6</sup>. Like other key transdiagnostic processes—and human behavior more broadly—craving results from brain function. However, it is typically assessed using subjective measures that require introspection and are sensitive to context<sup>6</sup>; thus, there is a strong need for biomarkers, and particularly neuromarkers, based on brain function<sup>36,37,44–46</sup>. Such biomarkers can identify mechanistic targets that can aid in monitoring disease progression (monitoring biomarkers according to the FDA), identifying individuals at risk for SUDs and future weight gain (prognostic biomarkers), predicting treatment response (predictive biomarkers) and serving as targets for neuromodulatory and behavioral interventions<sup>34</sup>.

In this study, we used machine learning to identify a distributed brain pattern—that we term the NCS as a reference for future use—that tracks the degree of craving when applied to new individuals, across different diagnostic groups, scanners and scanning parameters. Notably, this pattern separated drug users from non-users based on brain responses to drug cues but not food cues. Thus, it is an important step toward a diagnostic neuromarker of substance use. Furthermore,

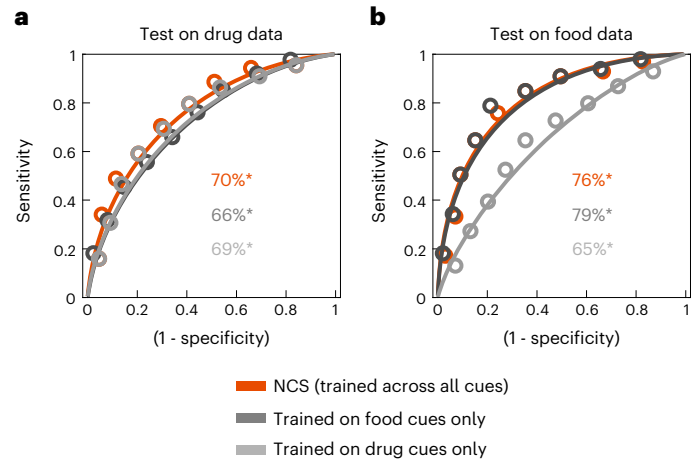


**Fig. 5 | Cross-prediction of drug craving and food craving based on drug-based and food-based brain patterns.** Compared to the NCS (trained across all conditions, red receiver operating characteristic plots), training on drug or food cues separately (gray receiver operating characteristic plots) does not improve accuracy, suggesting shared predictive patterns for cue-induced drug and food craving. Numbers indicate prediction accuracy for each brain classifier (all were significant, as indicated by stars).

given the role of self-reported craving in predicting outcomes<sup>4,5</sup>, this brain-based pattern may function as both a diagnostic and predictive biomarker with potential utility in predicting clinically relevant individual differences and future outcomes. Future studies could build on these findings to test whether the NCS responds to therapeutic interventions that reduce craving and/or drug use and whether it has predictive value for long-term clinical outcomes, such as drug relapse or weight gain. In addition, we found that the NCS is sensitive to cognitive regulation strategies, indicating that it may be psychologically modifiable. This is important because psychological and behavioral interventions can be effective for SUDs, but their mechanisms are poorly understood. Furthermore, current interventions are associated with high rates of relapse and could be improved<sup>47</sup>. Future models could also be developed based on other data types (for example, resting-state fMRI and imaging in animals) or their combination<sup>37,45</sup>.

Our results also offer new insight into a longstanding debate concerning the question whether craving of drugs and food share common

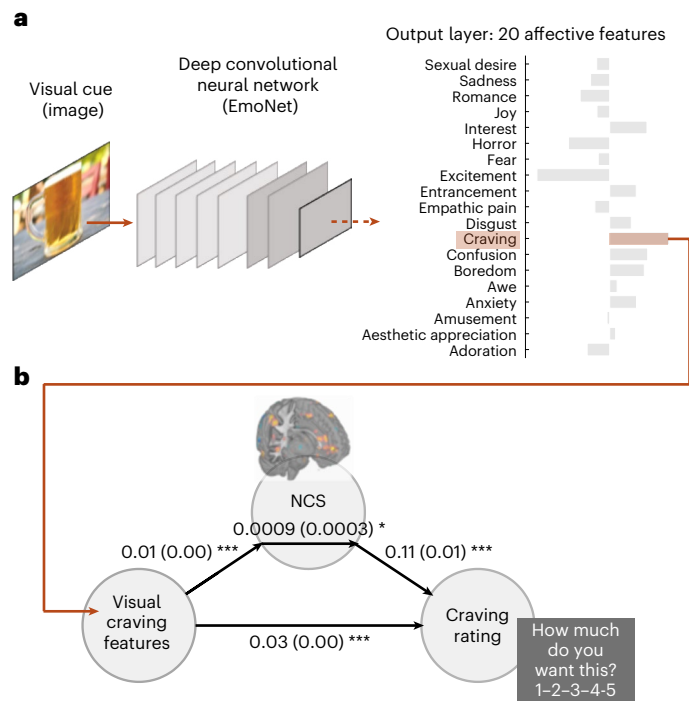


**Fig. 6 | The NCS partially mediates the effects of intrinsic visual craving features on craving ratings.** **a**, A deep convolutional neural network (EmoNet<sup>43</sup>, on the left) was used to extract visual craving-related features from the drug and food cue stimuli. We were most interested in the EmoNet ‘craving’ output, shaded in orange. **b**, A mediation analysis confirmed that (1) higher EmoNet ‘craving’ output was associated with higher NCS responses (path *a*,  $\beta = 0.01$ , STE = 0.00,  $P < 0.001$ ); (2) NCS responses significantly predicted craving ratings when controlling for visual features (path *b*,  $\beta = 0.11$ , STE = 0.01,  $P < 0.001$ ); and (3) the NCS partially mediated the effect of visual craving features on ratings (path *ab*,  $\beta = 0.0009$ , STE = 0.0003,  $P = 0.011$ ). Note that the direct path remained significant as well (path *c*,  $\beta = 0.03$ , STE = 0.00,  $P < 0.001$ ).

underlying brain processes, especially in motivation-related circuits<sup>39</sup>. We show that craving of various types of drugs and food can be predicted by largely shared whole-brain activity patterns. Indeed, the results demonstrate that craving-related responses to cues for legal and illegal drugs and for highly palatable food items are surprisingly similar and not dissociable at the fMRI pattern level in both drug-using and non-drug-using adults. This is noteworthy, especially as most of the non-users in the present studies were not obese or ‘food addicted’ but, rather, healthy controls. Notably, this overlap is consistent with models suggesting that drug craving depends on systems evolved for seeking highly palatable food and other primary rewards<sup>39</sup>. Future research could test whether the NCS also responds to less palatable or healthy food items and to other types of primary and secondary rewards.

Some areas in the NCS, including the vmPFC and VS/NAc, have been broadly implicated in reward and valuation<sup>48,49</sup> and have long been associated with craving and substance use across species. Several prior studies and meta-analyses<sup>38,40,50</sup> have demonstrated a central role of vmPFC, ventral striatum, amygdala, insula and posterior cingulate cortex in drug and food cue reactivity and craving (although findings across meta-analyses are inconsistent). The vmPFC has been targeted in repetitive transcranial magnetic stimulation (rTMS) studies to successfully reduce drug craving<sup>51</sup>. The positive peaks of the NCS in this area could, thus, serve as a more precise target for neurostimulation. Future studies can test whether successful neurostimulation of vmPFC also reduces NCS expression and alters connectivity of the vmPFC with other NCS core areas, such as the ventral striatum.

The insula is connected to many regions of the NCS and has been previously associated with craving<sup>52</sup>. Lesions in various insular locations have been shown to reduce the urge to use drugs and facilitate

smoking cessation<sup>53</sup>, which could reflect the role of the insula in the interoceptive component of drug craving<sup>54,55</sup>. The NCS has positive weights (at uncorrected thresholds) in the mid and posterior insula, in line with these previous reports. However, the anterior insula also displayed negative weights in the NCS (at uncorrected thresholds), revealing a potentially more complex role of different insula subregions in craving. Furthermore, the insula might be more prominent to bodily cues of withdrawal, craving and negative affect<sup>52</sup>, as well as for nutrient-related reward signals<sup>56</sup>, whereas areas such as amygdala or vmPFC (which are more prominent in the NCS) are related to craving evoked by external cues<sup>52</sup>, such as those employed in the present datasets.

The NCS’s weights were largely negative in lateral prefrontal cortex, lateral parietal areas, somatosensory cortex and precuneus, indicating that activity in these areas is associated with reduced craving. Lateral prefrontal cortex, particularly, is known to be involved in cognitive control and emotion regulation<sup>57</sup>, including the cognitive Regulation of Craving (for example, as shown previously in the same datasets<sup>58,59</sup>) and by others<sup>60–63</sup>. This area is also involved in the regulation of dietary decision-making, such as when focusing more on health aspects and long-term consequences of foods<sup>64</sup>. The negative weights of the NCS in these areas are, thus, consistent with these previous findings and recent simulation studies<sup>65</sup> that suggest a causal role for lateral prefrontal cortex in the regulation of drug and food craving.

Finally, predictive NCS features were also found in occipital and parietal brain areas associated with visual processing and attention allocation. Our control analyses demonstrated that those effects may not be due to differences in low-level visual stimulus features. The application of a deep neural network<sup>43</sup> showed that both behavioral craving ratings and NCS responses were partially driven by complex, craving-related stimulus features, as captured by EmoNet’s ‘Craving’ output. However, the NCS was associated with craving ratings above and beyond elementary and craving-related image features and partially mediated their effects on ratings, ruling out that this association was driven purely or primarily by low-level or complex image features or content. We also note that NCS weights in visual and attentional areas may reflect the effects of recurrent connections and top-down (content-related and meaning-related) effects on visual processing.

In sum, the NCS further extends prior work in several ways. First, it includes strong positive and negative weights in brain areas not previously associated with craving, such as the cerebellum and lateral temporal and parietal areas. These areas are connected to regions more traditionally associated with craving and might constitute new targets for investigation and intervention. Second, the NCS is a precise and replicable pattern, including relative activity levels across voxels within key regions and relative activity across networks. Thus, it constitutes a reproducible brain model<sup>30,66</sup> of craving that can be empirically quantified and validated in any new brain imaging study or dataset.

The present findings have some limitations that could be addressed in future studies. The included studies used a limited set of highly appetitive cues. Future studies could use a larger range of stimuli, including less palatable (and healthier) food items or non-craving-related (neutral) cues. Greater variation in craving ratings should, in principle, lead to increased discrimination accuracy between low and high craving. We also note that hunger ratings were available in Study 2 and did not correlate with NCS responses. Nevertheless, future work is needed to characterize how hunger or food deprivation modulates NCS responses to food (and other) cues or how NCS responses might differ in overweight or obese participants. Future studies could also test other modalities of drug and food cues (such as cigarette smoke or food smells and videos). The present study used craving ratings as the predicted outcome and did not have a non-craving control condition in the same group of participants. Although our supplemental analyses show that the NCS is distinct from other signatures that predict other types of affect ratings, the discriminant validity of the

NCS should be further evaluated in future studies. Another important future direction will be to validate whether the NCS predicts other correlates of craving, such as psychophysiological responses to drug cues, event-related potentials<sup>67</sup> and other types of behavioral measures<sup>68</sup>. In addition, fMRI has an inherently limited spatial resolution that cannot pinpoint the cellular or microstructural processes associated with craving or different types of craving. However, craving cannot be directly assessed in animals, and this work fills a crucial gap across species and brain systems, which is important for translating neuroscientific findings for human clinical use. It is also important for future translational applications of MRI-based neuromarkers, which will inevitably use different scanners, hardware and processes that evolve over time, thus requiring a focus on large-scale patterns that are generalizable across studies, scanners, groups, different pre-processing protocols and other factors.

In both Western and Eastern philosophy, craving has been considered a source of suffering and unhappiness. Although craving is an important feature of SUDs, eating disorders and other psychiatric conditions, it is also a general aspect of human experience. Identifying the neurobiological basis of this important driver of human behavior is, thus, an important step in mapping brain circuits to basic affective and mental processes. Here we introduced the NCS—to our knowledge, the first fMRI-based neuromarker of drug and food craving—which classifies drug users from non-users based on responses to drug but not food cues. As such, it offers a promising target for future research and clinical interventions.

### Online content

Any methods, additional references, Nature Portfolio reporting summaries, source data, extended data, supplementary information, acknowledgements, peer review information; details of author contributions and competing interests; and statements of data and code availability are available at <https://doi.org/10.1038/s41593-022-01228-w>.

### References

- O'Brien, C. P., Childress, A. R., Ehrman, R. & Robbins, S. J. Conditioning factors in drug abuse: can they explain compulsion? *J. Psychopharmacol.* **12**, 15–22 (1998).
- Janssen, F., Trias-Llimós, S. & Kunst, A. E. The combined impact of smoking, obesity and alcohol on life-expectancy trends in Europe. *Int. J. Epidemiol.* **50**, 931–941 (2021).
- Diagnostic and Statistical Manual of Mental Disorders* 5th ed. <https://dsm.psychiatryonline.org/doi/book/10.1176/appi.books.9780890425596> (2013).
- Vafaie, N. & Kober, H. Association of drug cues and craving with drug use and relapse: a systematic review and meta-analysis. *JAMA Psychiatry* **79**, 641–650 (2022).
- Boswell, R. G. & Kober, H. Food cue reactivity and craving predict eating and weight gain: a meta-analytic review. *Obes. Rev.* **17**, 159–177 (2016).
- Sayette, M. A. The role of craving in substance use disorders: theoretical and methodological issues. *Annu. Rev. Clin. Psychol.* **12**, 407–433 (2016).
- Jasinska, A. J., Stein, E. A., Kaiser, J., Naumer, M. J. & Yalachkov, Y. Factors modulating neural reactivity to drug cues in addiction: a survey of human neuroimaging studies. *Neurosci. Biobehav. Rev.* **38**, 1–16 (2014).
- Heilig, M. et al. Addiction as a brain disease revised: why it still matters, and the need for consilience. *Neuropsychopharmacology* **46**, 1715–1723 (2021).
- Berridge, K. C. & Robinson, T. E. Liking, wanting, and the incentive-sensitization theory of addiction. *Am. Psychol.* **71**, 670–679 (2016).
- Bedi, G. et al. Incubation of cue-induced cigarette craving during abstinence in human smokers. *Biol. Psychiatry* **69**, 708–711 (2011).
- Schoenbaum, G. & Shaham, Y. The role of orbitofrontal cortex in drug addiction: a review of preclinical studies. *Biol. Psychiatry* **63**, 256–262 (2008).
- Everitt, B. J., Dickinson, A. & Robbins, T. W. The neuropsychological basis of addictive behaviour. *Brain Res. Brain Res. Rev.* **36**, 129–138 (2001).
- Lüscher, C., Robbins, T. W. & Everitt, B. J. The transition to compulsion in addiction. *Nat. Rev. Neurosci.* **21**, 247–263 (2020).
- Farr, O. M., Li, C.-S. R. & Mantzoros, C. S. Central nervous system regulation of eating: insights from human brain imaging. *Metabolism* **65**, 699–713 (2016).
- Plassmann, H., Schelski, D. S., Simon, M.-C. & Koban, L. How we decide what to eat: toward an interdisciplinary model of gut-brain interactions. *Wiley Interdiscip. Rev. Cogn. Sci.* **13**, e1562 (2022).
- Schmidt, L. et al. Resting-state connectivity within the brain's reward system predicts weight loss and correlates with leptin. *Brain Commun.* **3**, fcab005 (2021).
- Lawrence, N. S., Hinton, E. C., Parkinson, J. A. & Lawrence, A. D. Nucleus accumbens response to food cues predicts subsequent snack consumption in women and increased body mass index in those with reduced self-control. *Neuroimage* **63**, 415–422 (2012).
- Ekhtiari, H. et al. Transcranial electrical and magnetic stimulation (tES and TMS) for addiction medicine: a consensus paper on the present state of the science and the road ahead. *Neurosci. Biobehav. Rev.* **104**, 118–140 (2019).
- Venniro, M., Banks, M. L., Heilig, M., Epstein, D. H. & Shaham, Y. Improving translation of animal models of addiction and relapse by reverse translation. *Nat. Rev. Neurosci.* **21**, 625–643 (2020).
- Whelan, R. & Garavan, H. When optimism hurts: inflated predictions in psychiatric neuroimaging. *Biol. Psychiatry* **75**, 746–748 (2014).
- Krishnan, A. et al. Somatic and vicarious pain are represented by dissociable multivariate brain patterns. *eLife* **5**, e15166 (2016).
- Woo, C.-W. et al. Separate neural representations for physical pain and social rejection. *Nat. Commun.* **5**, 5380 (2014).
- Wager, T. D. et al. An fMRI-based neurologic signature of physical pain. *N. Engl. J. Med.* **368**, 1388–1397 (2013).
- Kay, K. N., Naselaris, T., Prenger, R. J. & Gallant, J. L. Identifying natural images from human brain activity. *Nature* **452**, 352–355 (2008).
- Huth, A. G., Nishimoto, S., Vu, A. T. & Gallant, J. L. A continuous semantic space describes the representation of thousands of object and action categories across the human brain. *Neuron* **76**, 1210–1224 (2012).
- Rissman, J., Greely, H. T. & Wagner, A. D. Detecting individual memories through the neural decoding of memory states and past experience. *Proc. Natl Acad. Sci. USA* **107**, 9849–9854 (2010).
- Rosenberg, M. D. et al. A neuromarker of sustained attention from whole-brain functional connectivity. *Nat. Neurosci.* **19**, 165–171 (2016).
- Huth, A. G., de Heer, W. A., Griffiths, T. L., Theunissen, F. E. & Gallant, J. L. Natural speech reveals the semantic maps that tile human cerebral cortex. *Nature* **532**, 453–458 (2016).
- Eisenbarth, H., Chang, L. J. & Wager, T. D. Multivariate brain prediction of heart rate and skin conductance responses to social threat. *J. Neurosci.* **36**, 11987–11998 (2016).
- Kragel, P. A., Koban, L., Barrett, L. F. & Wager, T. D. Representation, pattern information, and brain signatures: from neurons to neuroimaging. *Neuron* **99**, 257–273 (2018).
- Reddan, M. C., Lindquist, M. A. & Wager, T. D. Effect size estimation in neuroimaging. *JAMA Psychiatry* **74**, 207–208 (2017).

32. Gabrieli, J. D. E., Ghosh, S. S. & Whitfield-Gabrieli, S. Prediction as a humanitarian and pragmatic contribution from human cognitive neuroscience. *Neuron* **85**, 11–26 (2015).
33. Davis, K. D. et al. Discovery and validation of biomarkers to aid the development of safe and effective pain therapeutics: challenges and opportunities. *Nat. Rev. Neurol.* **16**, 381–400 (2020).
34. FDA-NIH Biomarker Working Group. *BEST (Biomarkers, Endpoints, and other Tools)*. <https://www.ncbi.nlm.nih.gov/books/NBK326791/> (US Food & Drug Administration, 2016).
35. Knutson, B. & Genevsky, A. Neuroforecasting aggregate choice. *Curr. Dir. Psychol. Sci.* **27**, 110–115 (2018).
36. Volkow, N. D., Koob, G. & Baler, R. Biomarkers in substance use disorders. *ACS Chem. Neurosci.* **6**, 522–525 (2015).
37. Steele, V. R. et al. Machine learning of functional magnetic resonance imaging network connectivity predicts substance abuse treatment completion. *Biol. Psychiatry Cogn. Neurosci. Neuroimaging* **3**, 141–149 (2018).
38. Noori, H. R., Cosa Linan, A. & Spanagel, R. Largely overlapping neuronal substrates of reactivity to drug, gambling, food and sexual cues: a comprehensive meta-analysis. *Eur. Neuropsychopharmacol.* **26**, 1419–1430 (2016).
39. Volkow, N. D., Wise, R. A. & Baler, R. The dopamine motive system: implications for drug and food addiction. *Nat. Rev. Neurosci.* **18**, 741–752 (2017).
40. Tang, D. W., Fellows, L. K., Small, D. M. & Dagher, A. Food and drug cues activate similar brain regions: a meta-analysis of functional MRI studies. *Physiol. Behav.* **106**, 317–324 (2012).
41. Ziauddeen, H., Farooqi, I. S. & Fletcher, P. C. Obesity and the brain: how convincing is the addiction model? *Nat. Rev. Neurosci.* **13**, 279–286 (2012).
42. Ćeko, M., Kragel, P. A., Woo, C.-W., López-Solà, M. & Wager, T. D. Common and stimulus-type-specific brain representations of negative affect. *Nat. Neurosci.* **25**, 760–770 (2022).
43. Kragel, P. A., Reddan, M. C., LaBar, K. S. & Wager, T. D. Emotion schemas are embedded in the human visual system. *Sci. Adv.* **5**, eaaw4358 (2019).
44. Cosme, D., Zeithamova, D., Stice, E. & Berkman, E. T. Multivariate neural signatures for health neuroscience: assessing spontaneous regulation during food choice. *Soc. Cogn. Affect. Neurosci.* **15**, 1120–1134 (2020).
45. Whelan, R. et al. Neuropsychosocial profiles of current and future adolescent alcohol misusers. *Nature* **512**, 185–189 (2014).
46. Kühn, S. et al. Predicting development of adolescent drinking behaviour from whole brain structure at 14 years of age. *eLife* **8**, e44056 (2019).
47. Potenza, M. N., Sofuoglu, M., Carroll, K. M. & Rounsaville, B. J. Neuroscience of behavioral and pharmacological treatments for addictions. *Neuron* **69**, 695–712 (2011).
48. Bartra, O., McGuire, J. T. & Kable, J. W. The valuation system: a coordinate-based meta-analysis of BOLD fMRI experiments examining neural correlates of subjective value. *Neuroimage* **76**, 412–427 (2013).
49. Kable, J. W. & Glimcher, P. W. The neural correlates of subjective value during intertemporal choice. *Nat. Neurosci.* **10**, 1625–1633 (2007).
50. Kühn, S. & Gallinat, J. Common biology of craving across legal and illegal drugs—a quantitative meta-analysis of cue-reactivity brain response. *Eur. J. Neurosci.* **33**, 1318–1326 (2011).
51. Hanlon, C. A. et al. What goes up, can come down: novel brain stimulation paradigms may attenuate craving and craving-related neural circuitry in substance dependent individuals. *Brain Res.* **1628**, 199–209 (2015).
52. Naqvi, N. H., Gaznick, N., Tranel, D. & Bechara, A. The insula: a critical neural substrate for craving and drug seeking under conflict and risk. *Ann. N Y Acad. Sci.* **1316**, 53–70 (2014).
53. Naqvi, N. H., Rudrauf, D., Damasio, H. & Bechara, A. Damage to the insula disrupts addiction to cigarette smoking. *Science* **315**, 531–534 (2007).
54. Garavan, H. Insula and drug cravings. *Brain Struct. Funct.* **214**, 593–601 (2010).
55. Bud Craig, A. D. How do you feel—now? The anterior insula and human awareness. *Nat. Rev. Neurosci.* **10**, 59–70 (2009).
56. de Araujo, I. E., Schatzker, M. & Small, D. M. Rethinking food reward. *Annu. Rev. Psychol.* **71**, 139–164 (2020).
57. Buhle, J. T. et al. Cognitive reappraisal of emotion: a meta-analysis of human neuroimaging studies. *Cereb. Cortex* **24**, 2981–2990 (2014).
58. Kober, H. et al. Prefrontal–striatal pathway underlies cognitive regulation of craving. *Proc. Natl Acad. Sci. USA* **107**, 14811–14816 (2010).
59. Suzuki, S. et al. Regulation of craving and negative emotion in alcohol use disorder. *Biol. Psychiatry Cogn. Neurosci. Neuroimaging* **5**, 239–250 (2020).
60. Goldstein, R. Z. & Volkow, N. D. Dysfunction of the prefrontal cortex in addiction: neuroimaging findings and clinical implications. *Nat. Rev. Neurosci.* **12**, 652–669 (2011).
61. Yokum, S. & Stice, E. Cognitive regulation of food craving: effects of three cognitive reappraisal strategies on neural response to palatable foods. *Int. J. Obes.* **37**, 1565–1570 (2013).
62. Giuliani, N. R., Mann, T., Tomiyama, A. J. & Berkman, E. T. Neural systems underlying the reappraisal of personally craved foods. *J. Cogn. Neurosci.* **26**, 1390–1402 (2014).
63. Silvers, J. A. et al. Curbing craving: behavioral and brain evidence that children regulate craving when instructed to do so but have higher baseline craving than adults. *Psychol. Sci.* **25**, 1932–1942 (2014).
64. Hutcherson, C. A., Plassmann, H., Gross, J. J. & Rangel, A. Cognitive regulation during decision making shifts behavioral control between ventromedial and dorsolateral prefrontal value systems. *J. Neurosci.* **32**, 13543–13554 (2012).
65. Steele, V. R. Transcranial magnetic stimulation as an interventional tool for addiction. *Front. Neurosci.* **14**, 592343 (2020).
66. Rosenberg, M. D. & Finn, E. S. How to establish robust brain–behavior relationships without thousands of individuals. *Nat. Neurosci.* **25**, 835–837 (2022).
67. Franken, I. H. A., Hulstijn, K. P., Stam, C. J., Hendriks, V. M. & van den Brink, W. Two new neurophysiological indices of cocaine craving: evoked brain potentials and cue modulated startle reflex. *J. Psychopharmacol.* **18**, 544–552 (2004).
68. Creswell, K. G. et al. Assessing cigarette craving with a squeeze. *Clin. Psychol. Sci.* **7**, 597–611 (2019).

**Publisher's note** Springer Nature remains neutral with regard to jurisdictional claims in published maps and institutional affiliations.

Springer Nature or its licensor (e.g. a society or other partner) holds exclusive rights to this article under a publishing agreement with the author(s) or other rightsholder(s); author self-archiving of the accepted manuscript version of this article is solely governed by the terms of such publishing agreement and applicable law.

© The Author(s), under exclusive licence to Springer Nature America, Inc. 2022

## Methods

### Participants

The present analysis used the pooled data from  $n = 99$  participants (33 females,  $M_{AGE} = 34.1$  years,  $SD_{AGE} = 10.8$ ) collected across three independent neuroimaging studies (five different participant groups and three scanners; Fig. 1 and Supplementary Table 1). Two additional participants in Study 1 were excluded in the original study and for the present analyses due to vomiting and not following task instructions. In Study 2, four additional participants were excluded in the original study and for the present analysis due to unanticipated claustrophobia and non-completion of the task, one due to providing false information during the screening, one due to no responses in some runs of the task, two due to having been scanned in the morning and one due to excessive movement artifacts. In Study 3, three participants in the user group were excluded due to not understanding or not completing the task, one due to high anxiety and large movement artifacts, one due to being a past but not current cocaine user and one control participant due to high cocaine craving. Other details regarding the methods and procedures as well as other results from these datasets, focusing on the effects of regulation on behavior and univariate brain responses, are<sup>58,59</sup> or will be (Schafer, Potenza & Kober, unpublished data) reported elsewhere.

Analyses reported here were not reported previously, and the three studies have not been previously combined. Across studies, participants were recruited using flyers and ads (in newspapers, online bulletin boards, etc.) from communities around Yale and Columbia universities. Participants were included in drug-using groups ( $n = 59$ ,  $M_{AGE} = 34.6$  years,  $SD_{AGE} = 11.2$ , 18 females) based on verified clinical measures (for example, structured clinical interviews for diagnosis and/or Fagerström test of nicotine dependence). Information on the severity and duration of use is presented in Supplementary Table 1. Individuals were included in 'healthy control' groups ( $n = 40$ ,  $M_{AGE} = 33.4$  years,  $SD_{AGE} = 10.5$ , 15 females) if they were (1) age-matched, sex-matched and race-matched to the SUD group in each respective study; (2) did not qualify for any SUD diagnosis or primary psychiatric diagnoses; and (3) did not regularly consume the substance of the SUD group in each respective study (that is, matched healthy controls for the cigarette-smoking group did not regularly smoke). Participants in the drug-use group in Study 1 were heavy daily smokers who smoked an average of 15.7 cigarettes every day. Participants in the drug-use groups in Studies 2 and 3 completed diagnostic interviews and fulfilled *Diagnostic and Statistical Manual of Mental Disorders*, Fourth Edition, criteria for SUD (alcohol and cocaine, respectively). None of the participants was recruited for a treatment study. In Studies 2 and 3, participants were excluded if they were seeking treatment for their drug use. Drug users did not significantly differ from non-users in age, sex or racial/ethnic background. Compared to non-users, drug (especially cocaine) users had significantly lower years of education (Supplementary Table 1; 15.5 years versus 14.0 years,  $P < 0.001$ ). We, therefore, checked that the resulting NCS was not related to education level above and beyond drug-use status.

To avoid alterations in brain responses and to ensure craving, we made sure that participants (drug users or controls) were not intoxicated and were drug-negative at the time of scanning. In Study 1 (cigarette smokers and their matched controls), participants were asked not to smoke, eat or drink for at least 2 hours before their study appointment (resulting in a 3–4-hour abstinence at the time of scanning). We then used a breathalyzer to measure exhaled carbon monoxide to verify that participants indeed abstained from smoking, as instructed. Questions were used to verify their abstinence from eating and drinking in the absence of suitable biological verification methods. In addition, participants completed a standard urine toxicology test before the scan to verify abstinence from other drugs (opioids, amphetamines, methamphetamines, cocaine, barbiturates, benzodiazepines, PCP (phencyclidine) and THC (the primary psychoactive ingredient in

marijuana)). Participants whose test results indicated recent drug or alcohol use were not scanned. In Study 2 (individuals with alcohol use disorder), participants were told to not drink alcohol since the night before and not to eat or drink anything for at least 2 hours before their study appointment. We then used a breathalyzer to measure exhaled alcohol (the most common proxy for blood alcohol level) to verify that participants indeed abstained from drinking alcohol, as instructed (questions were used to verify their abstinence from eating and non-alcohol drinking). In addition, participants completed a standard urine toxicology test before the scan to verify abstinence from other drugs. Again, participants whose test results indicated drug or alcohol use were not scanned. In Study 3 (individuals with cocaine use disorder and their matched controls), participants were part of a larger study and had spent the prior several nights on an inpatient research unit, where they did not have any access to drugs or alcohol. Drug (and alcohol) abstinence at the time of scan was, thus, verified by observation. They were also asked not to eat or drink for at least 2 hours before the study participation and were accompanied to the scan directly from the clinical research unit by a research assistant. Thus, no participant was intoxicated during the experiment.

All participants provided informed consent and were paid for their participation in the study. The studies were approved by the institutional review boards of Columbia and Yale universities and were conducted in compliance with all relevant ethical regulations.

### Regulation of Craving task

The Regulation of Craving task is designed to evoke cue-induced craving of drug and food stimuli and to test participants' ability to regulate craving<sup>58</sup>. Participants were shown images of drugs and food that were known to induce craving (Supplementary Tables 2–4; each image was shown only once, and order was randomized across and within participants). Additional analyses showed that luminance ( $\beta = 0.08$ ,  $STE = 0.02$ ,  $t(95) = 4.39$ ,  $P < 0.001$ , Cohen's  $d = 0.45$ ), but not stimulus entropy ( $\beta = 0.01$ ,  $STE = 0.02$ ,  $t(95) = 0.52$ ,  $P = 0.60$ ), was significantly associated with NCS responses. However, when controlling for low-level visual features (stimulus luminance and entropy), single-trial NCS responses were still significantly associated with craving ratings ( $\beta = 0.19$ ,  $STE = 0.02$ ,  $t(95) = 9.44$ ,  $P < 0.001$ , Cohen's  $d = 0.97$ ), suggesting that the NCS does not opportunistically rely on these features for prediction of craving ratings.

On each trial, participants were instructed to observe these images in one of two ways. The NOW condition served as a craving baseline, whereby participants were instructed to consider the immediate positive consequences of consuming the pictured drug or food. In the LATER condition, participants were instructed to employ a cognitive strategy drawn from cognitive-behavioral treatments for substance use and obesity and to consider the negative consequences of repeated consumption of the drug or food.

On each of 100 trials (50 drug trials and 50 food trials, presented in random order using E-Prime software), participants were presented with a 2-second instructional cue (NOW or LATER) followed by a 6-second presentation of the drug or food image. After a jittered delay period (approximately 3 seconds), participants indicated how much they craved the drug or food at that moment ('How much do you want this?') on a 1–5 Likert scale, on which 1 indicated the lowest ('not at all') and 5 the highest ('very much') level of craving. Trials were separated by jittered intervals that followed an exponential distribution, during which a fixation cross was displayed. Prior work<sup>69–71</sup> including the results from the pooled datasets<sup>58,59</sup> have confirmed that participants report less craving for food and drugs in the regulation (LATER) compared to the craving (NOW) condition.

### fMRI data acquisition and pre-processing

Data were collected on three different scanners at Columbia and Yale universities using different acquisition parameters. Data underwent

standard pre-processing in SPM (versions 5, 8 and 12) including slice time correction, realignment, motion correction, warping and smoothing with a 6-mm full width at half maximum (FWHM) kernel. No data censoring was used. Differences in acquisition and pre-processing across datasets are, in fact, helpful in the current context, as they ensure that our pooled findings are not dependent on such details<sup>30,72</sup>.

### fMRI single-trial models

For each participant, we first computed a first-level GLM using SPM8 and custom scripts (<https://github.com/canlab>). These models contained separate regressors for trials in the same condition and rating level (1–5) per run (modeled at 8-second duration each). One additional regressor was added to model activity related to ratings (3 seconds) across all trials. Furthermore, 24 movement regressors (estimates for displacement and rotation in three dimensions, their derivatives, squared movement estimates and derivatives of squared movement estimates) and spike regressors (based on the identification of global outliers, coded as 1 for the outlier timepoint and 0 for all other timepoints) were added as regressor of no interest to control for motion artifacts.

Next, we averaged the resulting  $\beta$ -images for each participant within each rating level. This resulted in up to five  $\beta$ -images per participant that reflected craving levels from 1 to 5, respectively. If a participant did not have any ratings at a given level, a map for that level was not created for that participant (18 participants had one missing craving level, and four participants had two missing levels). To bring all images to the same scale (thus increasing comparability across studies and scanners) and to reduce the impact of potential outliers, each trial-averaged  $\beta$ -image was scaled (divided) by the L2 norm. An inclusive gray matter mask was applied to exclude voxels that likely contain white matter or cerebrospinal fluid only.

### Training and cross-validation of the NCS

The resulting images for all five levels of craving for each training participant were then used for linear prediction of craving using LASSO-PCR<sup>73</sup> and default parameters (to avoid overfitting). LASSO-PCR is a machine learning algorithm that is well suited for prediction of continuous outcomes based on large feature sets, such as whole-brain imaging data, which are characterized by substantially higher number of potential predictive features (that is, voxels) than outcome data points (for example, rating levels by subjects) and by a non-independence of these features (that is, voxel activity is strongly covaried across regions and functional networks). LASSO-PCR avoids overfitting by first performing data reduction using principal component regression (PCR), thereby identifying brain networks that are characterized by high covariation of voxels. It then performs the LASSO algorithm, which reduces the contribution of less important or more unstable components by shrinking their regression weights toward zero. Voxel weights can be reconstructed based on their scores for the different components, thus rendering the resulting classifier interpretable and applicable to new datasets.

We used a ten-fold cross-validation procedure to evaluate the predictive accuracy of the classifier. Thus, we divided the data into ten folds that were stratified by studies.  $\beta$ -images of any given participant (corresponding to all levels of craving) were always held out in the same fold. In each iteration, the classifier was trained on the remaining data and then tested on the held-out data by calculating predicted level of craving (or 'NCS response') as the dot product of the trained NCS and each held-out  $\beta$ -image. This out-of-sample-predicted level of craving was used to assess differences in NCS responses between low and high craving ratings, experimental conditions (instruction and cue type) and drug users versus controls. Because NCS responses reflect predicted ratings, they are, in principle, on the same scale as craving ratings but not restricted to whole numbers between 1 and 5. For training and testing of drug-craving and food-craving patterns separately, the same procedure was repeated but using only either drug or food contrast images, respectively.

### Bootstrapping and thresholding

To assess the voxels with the most reliable positive or negative weights, we performed a bootstrap test. In total, 10,000 samples with replacements were taken from the paired brain and outcome data, and the LASSO-PCR was repeated for each bootstrap sample. Two-tailed, uncorrected *P* values were calculated for each voxel based on the proportion of weights above or below zero<sup>23,74</sup>. FDR correction was applied to *P* values to correct for multiple comparisons across the whole brain. Significant cortical clusters (Table 1) were automatically labeled using a multimodal cortical parcellation<sup>75</sup>; basal ganglia regions are based on ref. <sup>76</sup>; cerebellar regions are based on ref. <sup>77</sup>; and brainstem regions are based on a combination of studies. Large-scale network names are based on an established resting-state parcellation<sup>78</sup>.

### Permutation tests

Statistical significance of the cross-validated prediction accuracy was assessed using permutation tests. In each of 5,000 iterations, craving ratings within each cohort were randomly permuted, and training and cross-validation was performed on the permuted data to establish a null distribution for performance measures (mean square error, root-mean-square error, mean absolute error and prediction–outcome correlation). Observed performance measures were compared to these permutation-based null distributions to obtain non-parametric *P* values.

### Classification analyses

We used binary receiver operating characteristic plots to illustrate the ability of the NCS to separate high versus low levels of craving using forced-choice tests (Fig. 2), where pattern expression values (the dot product of the held-out  $\beta$ -images with the classifier weights) were compared for each participant's highest and lowest level of craving, and the higher value was chosen as the highest level of craving. To separate drug users from non-users (Fig. 4b and Supplementary Fig. 5), pattern expression values (separately for drug, food or drug>food contrasts) for each participant were submitted to a single-interval test, thresholded for optimal overall accuracy. AUC is provided as a thresholded-independent measure of classification performance. Binomial tests were used to assess the statistical significance of classification accuracy.

### Other statistical analyses

Data collection and analysis were not performed blinded to the conditions of the experiments. GLMs and *t*-tests were used to assess NCS effects while statistically controlling for potential confounds, such as age, sex, education, head motion and signals, from white matter and ventricles. GLMs and ANOVA were used to test the effects of regulation and cue type on behavioral ratings and NCS responses. Data distribution was assumed to be normal, but this was not formally tested. No statistical methods were used to pre-determine sample sizes, but our sample sizes are similar to those reported in previous publications<sup>23</sup>.

### Reporting summary

Further information on research design is available in the Nature Portfolio Reporting Summary linked to this article.

### Data availability

Data, meta-data and NCS weight maps are available for non-commercial aims at [https://github.com/canlab/Neuroimaging\\_Pattern\\_Masks/tree/master/Multivariate\\_signature\\_patterns/2022\\_Koban\\_NCS\\_Craving](https://github.com/canlab/Neuroimaging_Pattern_Masks/tree/master/Multivariate_signature_patterns/2022_Koban_NCS_Craving) and at <https://doi.org/10.6084/m9.figshare.21174256>.

### Code availability

MATLAB code for analyses is available at <https://github.com/canlab>. Custom code to train and apply the NCS is available at [https://github.com/canlab/Neuroimaging\\_Pattern\\_Masks/tree/master/Multivariate\\_signature\\_patterns/2022\\_Koban\\_NCS\\_Craving](https://github.com/canlab/Neuroimaging_Pattern_Masks/tree/master/Multivariate_signature_patterns/2022_Koban_NCS_Craving).

## References

69. Lopez, R. B., Ochsner, K. N. & Kober, H. Brief training in regulation of craving reduces cigarette smoking. *J. Subst. Abuse Treat.* **138**, 108749 (2022).
70. Naqvi, N. H. et al. Cognitive regulation of craving in alcohol-dependent and social drinkers. *Alcohol. Clin. Exp. Res.* **39**, 343–349 (2015).
71. Boswell, R. G., Sun, W., Suzuki, S. & Kober, H. Training in cognitive strategies reduces eating and improves food choice. *Proc. Natl Acad. Sci. USA* **115**, E11238–E11247 (2018).
72. Woo, C.-W., Chang, L. J., Lindquist, M. A. & Wager, T. D. Building better biomarkers: brain models in translational neuroimaging. *Nat. Neurosci.* **20**, 365–377 (2017).
73. Tibshirani, R. Regression shrinkage and selection via the Lasso. *J. R. Stat. Soc. Ser. B Stat. Methodol.* **58**, 267–288 (1996).
74. Wager, T. D., Atlas, L. Y., Leotti, L. A. & Rilling, J. K. Predicting individual differences in placebo analgesia: contributions of brain activity during anticipation and pain experience. *J. Neurosci.* **31**, 439–452 (2011).
75. Glasser, M. F. et al. A multi-modal parcellation of human cerebral cortex. *Nature* **536**, 171–178 (2016).
76. Pauli, W. M., O'Reilly, R. C., Yarkoni, T. & Wager, T. D. Regional specialization within the human striatum for diverse psychological functions. *Proc. Natl Acad. Sci. USA* **113**, 1907–1912 (2016).
77. Diedrichsen, J., Balsters, J. H., Flavell, J., Cussans, E. & Ramnani, N. A probabilistic MR atlas of the human cerebellum. *Neuroimage* **46**, 39–46 (2009).
78. Schaefer, A. et al. Local–global parcellation of the human cerebral cortex from intrinsic functional connectivity MRI. *Cereb. Cortex* **28**, 3095–3114 (2018).

## Acknowledgements

This work was funded by a grant from the National Institute on Drug Abuse (R01DA043690 to H.K.) and a Campus France Marie Skłodowska Curie co-fund fellowship (PRESTIGE-2018-2-0023 to L.K.). Collection of the datasets included herein was funded by R01DA022541 (principal investigator (PI): K. Ochsner), P50AA012870 (PI: J. Krystal) and P20DA027844 (PI: M. Potenza). We thank everyone who supported the collection of these data. We also thank N. Vafaie for help with data management and transfer.

## Author contributions

H.K. designed the experiments and collected the data. L.K. analyzed the data, created the figures and wrote the first draft of the manuscript. H.K. and T.W. conceived the project, obtained funding and supervised the project. All authors contributed to the writing and editing of the paper.

## Competing interests

None of the authors has competing financial or non-financial interests.

## Additional information

**Supplementary information** The online version contains supplementary material available at <https://doi.org/10.1038/s41593-022-01228-w>.

**Correspondence and requests for materials** should be addressed to Leonie Koban, Tor D. Wager or Hedy Kober.

**Peer review information** *Nature Neuroscience* thanks Elliot Stein, Sonja Yokum and the other, anonymous, reviewer(s) for their contribution to the peer review of this work.

**Reprints and permissions information** is available at [www.nature.com/reprints](http://www.nature.com/reprints).

## Reporting Summary

Nature Portfolio wishes to improve the reproducibility of the work that we publish. This form provides structure for consistency and transparency in reporting. For further information on Nature Portfolio policies, see our [Editorial Policies](#) and the [Editorial Policy Checklist](#).

### Statistics

For all statistical analyses, confirm that the following items are present in the figure legend, table legend, main text, or Methods section.

- | n/a                                 | Confirmed  |
|-------------------------------------|--|
| <input type="checkbox"/>            | <input checked="" type="checkbox"/> The exact sample size ( $n$ ) for each experimental group/condition, given as a discrete number and unit of measurement  |
| <input type="checkbox"/>            | <input checked="" type="checkbox"/> A statement on whether measurements were taken from distinct samples or whether the same sample was measured repeatedly  |
| <input type="checkbox"/>            | <input checked="" type="checkbox"/> The statistical test(s) used AND whether they are one- or two-sided<br><i>Only common tests should be described solely by name; describe more complex techniques in the Methods section.</i>   |
| <input type="checkbox"/>            | <input checked="" type="checkbox"/> A description of all covariates tested   |
| <input type="checkbox"/>            | <input checked="" type="checkbox"/> A description of any assumptions or corrections, such as tests of normality and adjustment for multiple comparisons  |
| <input type="checkbox"/>            | <input checked="" type="checkbox"/> A full description of the statistical parameters including central tendency (e.g. means) or other basic estimates (e.g. regression coefficient) AND variation (e.g. standard deviation) or associated estimates of uncertainty (e.g. confidence intervals) |
| <input type="checkbox"/>            | <input checked="" type="checkbox"/> For null hypothesis testing, the test statistic (e.g. $F$ , $t$ , $r$ ) with confidence intervals, effect sizes, degrees of freedom and $P$ value noted<br><i>Give <math>P</math> values as exact values whenever suitable.</i>                            |
| <input checked="" type="checkbox"/> | <input type="checkbox"/> For Bayesian analysis, information on the choice of priors and Markov chain Monte Carlo settings  |
| <input checked="" type="checkbox"/> | <input type="checkbox"/> For hierarchical and complex designs, identification of the appropriate level for tests and full reporting of outcomes  |
| <input type="checkbox"/>            | <input checked="" type="checkbox"/> Estimates of effect sizes (e.g. Cohen's $d$ , Pearson's $r$ ), indicating how they were calculated   |

*Our web collection on [statistics for biologists](#) contains articles on many of the points above.*

### Software and code

Policy information about [availability of computer code](#)

Data collection

Data analysis

For manuscripts utilizing custom algorithms or software that are central to the research but not yet described in published literature, software must be made available to editors and reviewers. We strongly encourage code deposition in a community repository (e.g. GitHub). See the Nature Portfolio [guidelines for submitting code & software](#) for further information.

### Data

Policy information about [availability of data](#)

All manuscripts must include a [data availability statement](#). This statement should provide the following information, where applicable:

- Accession codes, unique identifiers, or web links for publicly available datasets
- A description of any restrictions on data availability
- For clinical datasets or third party data, please ensure that the statement adheres to our [policy](#)

Data, meta-data, and NCS weight maps are available for non-commercial aims at: [https://github.com/canlab/Neuroimaging\\_Pattern\\_Masks/tree/master/Multivariate\\_signature\\_patterns/2022\\_Koban\\_NCS\\_Craving](https://github.com/canlab/Neuroimaging_Pattern_Masks/tree/master/Multivariate_signature_patterns/2022_Koban_NCS_Craving).

## Field-specific reporting

Please select the one below that is the best fit for your research. If you are not sure, read the appropriate sections before making your selection.

Life sciences       Behavioural & social sciences       Ecological, evolutionary & environmental sciences

For a reference copy of the document with all sections, see [nature.com/documents/nr-reporting-summary-flat.pdf](https://www.nature.com/documents/nr-reporting-summary-flat.pdf)

## Life sciences study design

All studies must disclose on these points even when the disclosure is negative.

Sample size	Sample size (N=99) was based on the availability of existing study data and is comparable with previous studies that have used a similar approach in other domains (e.g., Wager, 2013).
Data exclusions	All participants whose data has been included in the previous studies were also included for this manuscript. Two participants that were excluded in the original study on cigarette craving were also excluded in the present analysis.
Replication	Main effects of experimental conditions replicate across 3 cohorts of users and 2 cohorts of matched control participants. Classifier performance is assessed using cross-validation and replicates in all 5 cohorts. Separation of drug users versus non-users by the classifier was replicated across two studies. The classifier is available for future studies to test generalizability.
Randomization	Quasi-experimental groups: drug users versus non-users (randomization not possible). We statistically controlled for age, sex, education, and average head motion by adding these variables as covariates to a general linear model. Other factors were manipulated and randomly presented within-subjects in different trials (e.g., type of cue, regulation condition).
Blinding	Participant could not be blinded to their drug use status. Data acquisition and analysis were not blind to drug user status. Cue-type and regulation-condition were randomly presented in the scanner (without the presence of the experimenter)

## Reporting for specific materials, systems and methods

We require information from authors about some types of materials, experimental systems and methods used in many studies. Here, indicate whether each material, system or method listed is relevant to your study. If you are not sure if a list item applies to your research, read the appropriate section before selecting a response.

### Materials & experimental systems

n/a	Involved in the study
<input checked="" type="checkbox"/>	<input type="checkbox"/> Antibodies
<input checked="" type="checkbox"/>	<input type="checkbox"/> Eukaryotic cell lines
<input checked="" type="checkbox"/>	<input type="checkbox"/> Palaeontology and archaeology
<input checked="" type="checkbox"/>	<input type="checkbox"/> Animals and other organisms
<input type="checkbox"/>	<input checked="" type="checkbox"/> Human research participants
<input checked="" type="checkbox"/>	<input type="checkbox"/> Clinical data
<input checked="" type="checkbox"/>	<input type="checkbox"/> Dual use research of concern

### Methods

n/a	Involved in the study
<input checked="" type="checkbox"/>	<input type="checkbox"/> ChIP-seq
<input checked="" type="checkbox"/>	<input type="checkbox"/> Flow cytometry
<input type="checkbox"/>	<input checked="" type="checkbox"/> MRI-based neuroimaging

## Human research participants

Policy information about [studies involving human research participants](#)

Population characteristics	The present analysis used the pooled data from N=99 participants (33 female) collected across three independent neuroimaging studies (five different participant groups, three scanners, see Figure 1 and Table 3). Detailed methods and procedures as well as other results from these data sets, focusing on the effects of regulation on behavior and univariate brain responses, are reported elsewhere [74-76].
Recruitment	Participants were recruited using flyers and ads (in newspapers, online bulleting boards, etc.) from communities around Yale and Columbia Universities. Participants were included in drug using groups (N=59, MAGE=34.6 years, 18 female) based on verified clinical measures (e.g., structured clinical interviews for diagnosis and/or Fagerström test of nicotine dependence). Individuals were included in "healthy control" groups (N=40, MAGE=33.4 years, 15 female) if they were (1) age-, sex-, and race-matched to the SUD group in each respective study, (2) did not qualify for any SUD diagnosis or primary psychiatric diagnoses, and (3) did not regularly consume the substance of the SUD group in each respective study (i.e., matched healthy controls for the alcohol-using group did not regularly consume alcohol). Drug users recruited for this study from the New Haven and New York communities may not be representative of the entire population of drug users in these communities or those in other communities and countries.
Ethics oversight	All participants provided informed consent and were paid for their participation. The studies have been approved by the

Note that full information on the approval of the study protocol must also be provided in the manuscript.

## Magnetic resonance imaging

### Experimental design

Design type

event-related fMRI

Design specifications

On each of 80 or 100 trials (half drug, half food trials, presented in random order), participants were presented with a 2-second instructional cue (NOW or LATER) followed by a 6-second presentation of the drug or food image. After a jittered delay period (around 3 second), participants indicated how much they craved the drug or food at that moment ("How much do you want this?") on a 1-5 Likert scale, on which 1 indicated the lowest ("not at all") and 5 the highest ("very much") level of craving. Trials were separated by a jittered intertrial interval around 4s, during which a fixation cross was displayed.

Behavioral performance measures

Craving ratings (not performance-related)

### Acquisition

Imaging type(s)

fMRI

Field strength

3T

Sequence &amp; imaging parameters

Data were collected on three different scanners at Columbia and Yale Universities using different acquisition parameters (reported in previous publications).

Area of acquisition

Whole brain

Diffusion MRI

 Used Not used

### Preprocessing

Preprocessing software

SPM

Normalization

Functional images were co-registered to the structural image and warped to the Montreal Neurological Institute template

Normalization template

MNI template

Noise and artifact removal

Motion estimation using SPM, motion parameters, their squares and derivatives, as well as spike regressors for excessive movements were included in first-level models as regressors of no interest.

Volume censoring

No volume censoring was used.

### Statistical modeling & inference

Model type and settings

For each participant, we first computed a first level general linear model (GLM) using SPM8 and custom scripts ([canlab.github.org](https://github.com/canlab)). These models contained separate regressors for trials in the same condition and rating level (1-5), per run (modeled at 8s duration each). One additional regressor was added to model activity related to ratings (3s) across all trials. Further, 24 movement regressors (estimates for displacement and rotation in three dimensions, their derivatives, squared movement estimates, and derivatives of squared movement estimates) and spike regressors (based on the identification of global outliers, coded as 1 for the outlier time point and zero for all other time points) were added as regressor of no interest to control for motion artifacts.

Next, we averaged the resulting beta-images for each participant within each rating level. This resulted in up to five beta images per participant that reflected craving levels from 1 to 5, respectively (if a participant did not have any ratings at a given level, a map for that level was not created for that participant). In order to bring all images to the same scale (thus increasing comparability across studies and scanners) and reduce the impact of potential outliers, L2norming was applied to all averaged beta images. An inclusive gray-matter-masks was applied to exclude voxels that likely contain white matter or cerebrospinal fluid only.

The resulting images for each level of craving were then used for linear prediction of craving using LASSO-PCR (least absolute shrinkage and selection operator-principal component regression) and default parameters (to avoid overfitting). LASSO-PCR is a machine-learning algorithm that is well suited for prediction of outcomes based on large feature sets such as whole brain imaging data, which is characterized by substantially higher number of potential predictive features (i.e., voxels) than outcome data points (e.g., rating levels by subjects), and by a non-independence of these features (i.e., voxel activity is strongly covaried across regions and functional networks). LASSO-PCR avoids overfitting by first performing data reduction using principal component regression, thereby identifying brain networks that are characterized by high covariation of voxels. It then performs the LASSO algorithm, which reduces the contribution of less important or more unstable components by shrinking their regression weights towards zero. Voxel weights can be reconstructed based on their scores for the different components, thus rendering the resulting classifier interpretable and applicable to new datasets.

We used a 10-fold cross-validation procedure to evaluate the predictive accuracy of the classifier. Thus, we divided the data

into 10 folds that were stratified by studies. Beta images of any given participants (corresponding to all levels of craving) were always held out in the same fold. In each iteration, the classifier was trained on the remaining data and then tested on the hold out data by calculating predicted level of craving as the dot product of the trained NCS and each held out beta-image. This out-of-sample predicted level of craving was used to assess differences in NCS responses between low and high craving ratings, experimental conditions (instruction, cue type), and drug users versus controls. For training and testing of drug- and food-craving patterns separately, the same procedure was repeated, but only using either drug or food contrast images, respectively.

Effect(s) tested

Prediction of high versus low levels of craving (based on 1-5 ratings), drug users vs. not.

Specify type of analysis:  Whole brain  ROI-based  Both

Anatomical location(s) Gray-matter mask (whole brain)

Statistic type for inference  
(See [Eklund et al. 2016](#))

Prediction across the whole brain gray-matter. Voxel-based thresholding of most consistently positive or negative voxels.

Correction

FDR

## Models & analysis

n/a | Involved in the study

- Functional and/or effective connectivity  
  Graph analysis  
  Multivariate modeling or predictive analysis

Multivariate modeling and predictive analysis

The contrast images for each level of craving were used for linear prediction of craving using LASSO-PCR (least absolute shrinkage and selection operator-principal component regression) and default parameters (to avoid overfitting). LASSO-PCR is a machine-learning algorithm that is well suited for prediction of outcomes based on large feature sets such as whole brain imaging data, which is characterized by substantially higher number of potential predictive features (i.e., voxels) than outcome data points (e.g., rating levels by subjects), and by a non-independence of these features (i.e., voxel activity is strongly covaried across regions and functional networks). LASSO-PCR avoids overfitting by first performing data reduction using principal component regression, thereby identifying brain networks that are characterized by high covariation of voxels. It then performs the LASSO algorithm, which reduces the contribution of less important or more unstable components by shrinking their regression weights towards zero. Voxel weights can be reconstructed based on their scores for the different components, thus rendering the resulting classifier interpretable and applicable to new datasets.

We used a 10-fold cross-validation procedure to evaluate the predictive accuracy of the classifier. Thus, we divided the data into 10 folds that were stratified by studies. Beta images of any given participants (corresponding to all levels of craving) were always held out in the same fold. In each iteration, the classifier was trained on the remaining data and then tested on the hold out data by calculating predicted level of craving as the dot product of the trained NCS and each held out beta-image. This out-of-sample predicted level of craving was used to assess differences in NCS responses between low and high craving ratings, experimental conditions (instruction, cue type), and drug users versus controls. For training and testing of drug- and food-craving patterns separately, the same procedure was repeated, but only using either drug or food contrast images, respectively.